

# Small-molecule-mediated precision protein editing in living cells

Ge Sun<sup>1,2#</sup>, Jin Lin<sup>3#</sup>, Zhicheng Yang<sup>2#</sup>, Jie Yang<sup>4#</sup>, Yiran Hu<sup>2,5#</sup>, Fei Ye<sup>6#</sup>, Yizhou Bian<sup>3</sup>, Shuiping Fu<sup>2</sup>, Yifan Ma<sup>2</sup>, Zhenyu Wang<sup>2</sup>, Ziteng Li<sup>2</sup>, Junyi Qiu<sup>1</sup>, Hu Zhou<sup>\*2</sup>, Hua Lin<sup>\*4</sup>, Cheng Luo<sup>\*1,2,3,5</sup>

<https://doi.org/10.15302/vita.2026.03.0020>

Dear Editor,

The ability to directly and precisely manipulate native proteins without altering their underlying genetic code represents a longstanding unmet challenge in chemical biology. While genome editing technologies have revolutionized biology<sup>1,2</sup>, a key gap remains: the lack of methods for direct, site-specific single amino acid editing in endogenous proteins<sup>3</sup>. Existing protein-level strategies — such as split inteins<sup>4,5</sup> or chemical post-translational modifications<sup>6,7</sup> typically require overexpression of exogenous tags and lack true residue-level specificity. Here we develop light-induced Asp(D)-to-Ala(A) protein editors (LIDAPEs) which enable site-specific residue transformation in living cells, and lay the foundation for a new class of chemical biology tools.

The conserved DFG motif is critical for kinase catalytic activity<sup>8,9</sup> (Supplementary Fig. S1). Evidence shows that mutating the catalytic aspartate to a non-acidic residue, such as alanine, abolishes kinase activity<sup>10</sup>. This inherent sensitivity makes kinases a readily tractable substrate for D-to-A single-residue editing. Demonstrating this edit would provide compelling proof that native protein editing has been achieved with true residue-level precision (Fig. 1a).

In chemical terms, D-to-A single-residue editing proceeds through hydrodecarboxylation of the aspartate side chain. However, selectively modifying a single carbon-carbon bond within a native protein is highly challenging as the editing must discriminate the target side chain from all other acidic groups, particularly the protein's C-terminus which is intrinsically more reactive than an aspartate side chain<sup>11</sup>. Inspired by natural enzymatic systems, we turned to *Chlorella variabilis* fatty acid photodecarboxylase (FAP), an enzyme that efficiently hydrodecarboxylates fatty acids in a light-dependent manner. FAP employs a flavin adenine dinucleotide (FAD) cofactor to absorb visible light and drives the hydrodecarboxylation process (Fig. 1b). Examination of its active site reveals the sophisticated nature of this system: a pre-organized environment in which key water molecules mediate interactions between FAD and the substrate, thereby enabling precise substrate positioning and efficient electron and proton transfer (Fig. 1b, right panel)<sup>12</sup>. Accordingly, we developed a LIDAPE that integrates ligand-based kinase recognition (binder) with a light-induced catalytic D-to-A transformation (warhead).

To realize the LIDAPE system in practice, we developed a

new bio-compatible system capable of converting aspartic acid derivatives and Asp-containing peptides into the corresponding side-chain hydrodecarboxylation products (Supplementary Fig. S2a). We began by screening individual organophotocatalysts (PCs) for this transformation under aqueous-compatible conditions. Among the catalysts screened, riboflavin (PC-1) and 1,4-dicyanobenzene (DCB, PC-2) produced only trace amounts of the desired alanine product<sup>13</sup>. In contrast, 7-hydroxy-2-oxo-2H-chromene-3-carbonitrile (PC-3) afforded a 5% yield (Fig. 1c). Intriguingly, the molecular scaffold of PC-3 shares pronounced similarity to key pharmacophores found in kinase inhibitors, which prompted us to evaluate a representative kinase inhibitor core, PC-4, as a potential catalyst (Fig. 1c, upper panel). The substitution proved beneficial, with PC-4 delivering a markedly improved yield of 10%.

However, the exogenous base (1-acetylguanidine) remained a major limitation for protein-level applications (Supplementary Table S1, entry 3). To address this constraint, we designed integrated catalysts LL-DA-1 and LL-DA-2 by appending a guanidine moiety to the PC-4 core, inspired by the FAP system. Both catalysts effectively promoted the reaction, delivering 21% and 23% yields, respectively. When applied to a model Asp-containing dipeptide, these systems showed good compatibility with the small peptide, affording slightly improved conversions of 25% and 26%, respectively (Fig. 1c, lower panel).

Next, based on our interest in cyclin-dependent protein kinase (CDK) modulators<sup>14,15</sup>, we selected CDK2 for molecular docking as it features a well-defined ATP-binding pocket and a conserved DFG motif. LL-DA-1 docked into the ATP-binding pocket of CDK2, positioning the critical cyano and carbonyl group in close proximity to the target side chain Asp145 residue, consistent with the potential to mediate selective hydrodecarboxylation of the target residue within the kinase (Fig. 1c, middle panel).

Given these, LL-DA-1 and LL-DA-2 were screened against a panel of 77 kinases (Supplementary Figs. S3, S4). At 100  $\mu$ M, CDK2 emerged as the top hit, exhibiting 90–100% inhibition. We then applied both compounds to site-selective editing of three kinases with varied levels of inhibition: CDK2 (90–100%), CDK12 (70–80%), and FGFR2 (50–70%), targeting specific aspartate residues. LL-DA-1 outperformed LL-DA-2 in achieving 17.6% conversion of CDK2 D145 to A145, 2.6% effi-

1. State Key Laboratory of Discovery and Utilization of Functional Components in Traditional Chinese Medicine, Guizhou Provincial Key Laboratory of Digestive System Diseases, The Affiliated Hospital of Guizhou Medical University, Guiyang, Guizhou, China. 2. State Key Laboratory of Drug Research, Shanghai Institute of Materia Medica, Chinese Academy of Sciences, Shanghai, China. 3. The School of Pharmacy, Fujian Medical University, Fuzhou, Fujian, China. 4. Key Laboratory of Microbial Pathogenesis and Interventions of Fujian Province University, the Key Laboratory of Innate Immune Biology of Fujian Province, Biomedical Research Center of South China, College of Life Sciences, Fujian Normal University, Fuzhou, Fujian, China. 5. Hangzhou Institute for Advanced Study, University of Chinese Academy of Sciences, Hangzhou, Zhejiang, China. 6. College of Life Sciences and Medicine, Zhejiang Sci-Tech University, Hangzhou, Zhejiang, China. # These authors contributed equally. \*Correspondence: Hu Zhou ([zhouhu@simmm.ac.cn](mailto:zhouhu@simmm.ac.cn)), Hua Lin ([hlin@fjnu.edu.cn](mailto:hlin@fjnu.edu.cn)), Cheng Luo ([cluo@simmm.ac.cn](mailto:cluo@simmm.ac.cn))

Received: November 25, 2025; Accepted: March 18, 2026; Published: April 1, 2026

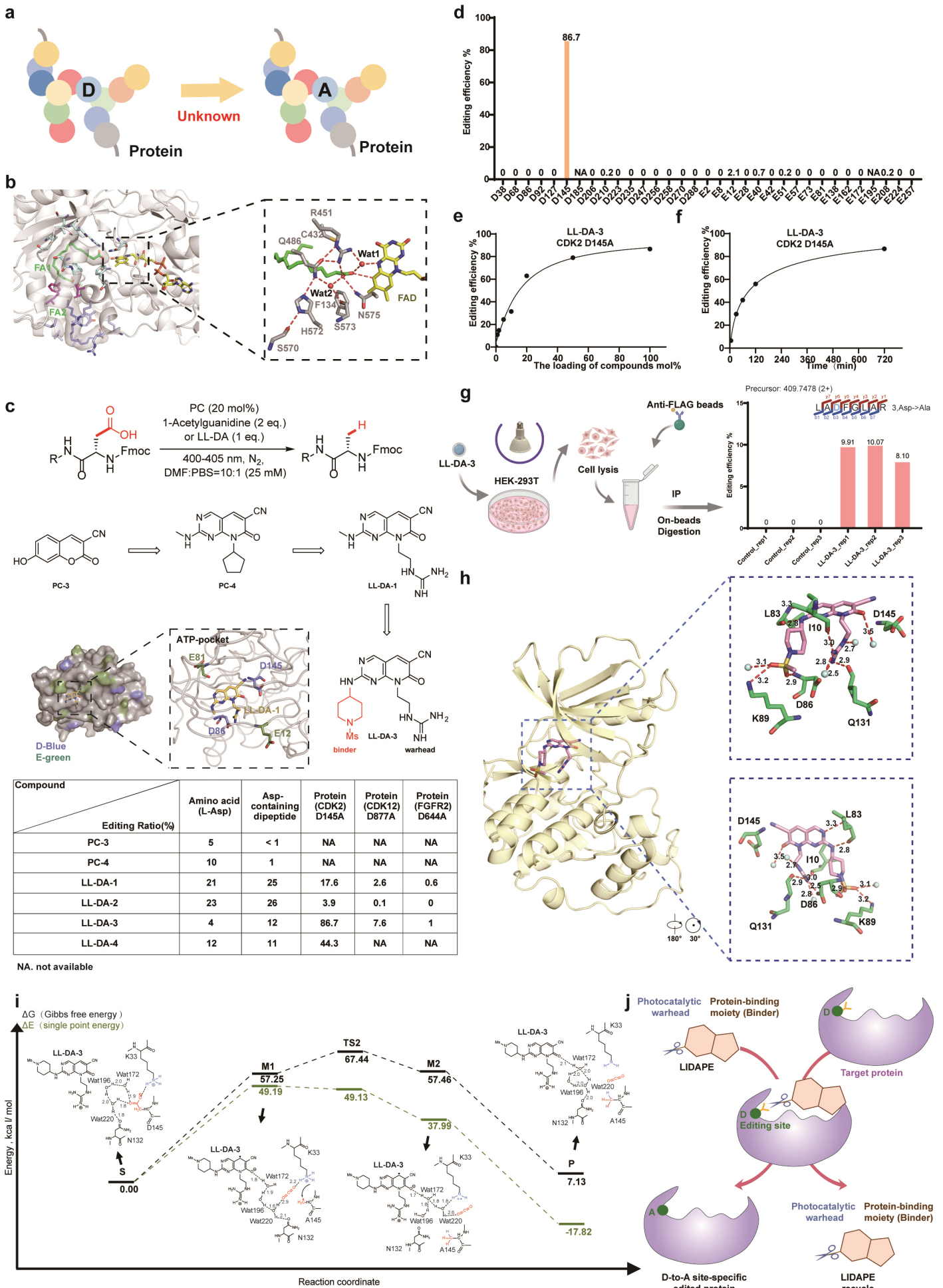


**Fig. 1 Design and characterization of the LIDAPE platform.** **a** Protein level D-to-A editing. **b** Structure of CvFAP including the FAD cofactor and two C18 fatty acid substrates (FA1 and FA2). The structural representation is based on data published by Sorigué *et al.* (PDB: 6YRU)<sup>12</sup>. **c** Screening and optimization of LIDAPEs for efficient hydrodecarboxylation. The middle panel: docking model of LL-DA-1 (yellow sticks) and CDK2. The lower panel: Editing efficiency of LIDAPEs. **d** The editing efficiency of LL-DA-3 across all D and E sites on CDK2. **e** Editing efficiency of LL-DA-3 at varied compound concentrations. **f** Time-dependent editing efficiency of LL-DA-3 on CDK2. **g** D145A editing of CDK2 by LL-DA-3. The edited peptide appeared only in LL-DA-3 samples, while vehicle controls showed none. **h** Overall view and detailed binding interactions of the crystal structure of CDK2 binding with LL-DA-3 (pink sticks). All distances are given in Ångstroms. **i** The possible photoreaction pathways according to quantum chemistry calculations. **j** State-of-the-art protein editing approach.

ciency at D877 of CDK12, and 0.6% at D644 of FGFR2 (Supplementary Fig. S5). LL-DA-2 demonstrated lower editing efficiency with 3.9% conversion of CDK2 D145A, trace editing of CDK12 and FGFR2. These results reveal a lack of direct correlation between kinase inhibition and editing efficiency (Supplementary Figs. S3–S5). Notably, LL-DA-1 showed both higher inhibition and editing efficiency for CDK2 and CDK12, whereas for FGFR2, LL-DA-2 exhibited stronger inhibition but lower editing efficiency. Together, these findings suggest that even in cases of modest kinase inhibition, targeted editing of specific aspartate residues is achievable.

Profiling across the CDK2 sequence after LL-DA-1 editing confirmed its high specificity, as evidenced by tryptic digest analysis followed by liquid chromatography-tandem mass spectrometry (LC-MS/MS). Among the D and E residues detectable by LC-MS/MS, only D127 and E51 exhibited minimal reactivity (0.1%) with LL-DA-1 (Supplementary Fig. S6a). Importantly, residues such as D127 and E12 located within the binding pocket remained largely unmodified, and the intrinsically more reactive C-terminal acidic group was also unaltered. Further support came from identification of the edited peptide LAAFGLAR, detected as a doubly charged precursor ion ( $[M+2H]^{2+}$  at  $m/z$  409.7478), exhibiting a 43.9898 Da decrease in monoisotopic mass, consistent with the D145A substitution (Supplementary Fig. S6b). Searches using pFind, Skyline, BiopharmFinder, and MaxQuant consistently identified the edited peptide exclusively at D145 with  $\leq 1\%$  peptide-level false discovery rate, confirming the high precision of LIDAPE (Supplementary Fig. S6c).

Given the high editing efficiency of the LIDAPEs, we next employed these catalysts as warheads to develop more potent CDK2-targeted LIDAPEs. Replacement of the methyl amine group with 1-(methylsulfonyl)piperidin-4-amine, a CDK2 specific binder, yielded LL-DA-3 and LL-DA-4 with enhanced binding affinity toward CDK2 (Fig. 1c; Supplementary Figs. S7a and S10). Notably, LL-DA-3 converted CDK2 D145 to A145 with 86.7% efficiency. LL-DA-4 achieved 44.3% (Fig. 1c, lower panel). Then, we profiled editing across all aspartate, glutamate residues and C-terminal acidic groups in CDK2. Editing was confined exclusively at D145. No other acidic residues were significantly modified (Fig. 1d). This level of precision is unprecedented for a small-molecule-mediated reaction in a full-length protein.

We next evaluated the wavelength compatibility of the LIDAPE. The result showed that wavelengths ranging from 370 nm to 405 nm effectively induced high editing efficiencies, surpassing 70% (Supplementary Fig. S7b). This observation is consistent with the absorbance spectra (Supplementary Fig. S7c). The UV-visible spectrum of LL-DA-3 exhibited an absorption peak at 374 nm, while its fluorescence emission peak was observed at 410 nm, which closely aligns with the light source wavelength range (400–405 nm). In addition, cyclic voltammetry measurements revealed a reduction half-peak potential ( $E_{1/2}^{\text{red}}$ ) of  $-0.728$  V (vs Ag/AgCl) for LL-DA-3 in DMF (Supplementary Fig. S7d). Based on these results, the

reduction potential of the excited state ( $E_{1/2}^{*\text{red}}$ ) for LL-DA-3 was calculated to be 2.292 V (vs Ag/AgCl, Supplementary Table S3), which is significantly more positive than the aspartic acid side chain.

A key feature of enzymes is their catalytic capability. We asked whether LL-DA-3 could function catalytically at the protein level. Editing efficiency depended on the concentration of LL-DA-3. Using only 1 mol% of LL-DA-3 still yielded 10.9% edited product. Further increases in compound loading led to even higher editing efficiency. This confirmed multiple turnover events (Fig. 1e). The reaction proceeded in a time-dependent manner (Fig. 1f) and was compatible with physiological reductants (Supplementary Tables S4 and S5). To mimic the binding of LL-DA-3 to CDK2 before and after editing, Bio-Layer Interferometry experiments were conducted. The results showed that compared to wild-type CDK2, the D145A variant of CDK2 had significantly weaker binding to LL-DA-3 and a faster dissociation rate (Supplementary Fig. S8). This indicated that once editing was completed, the compound preferentially bound to the unedited protein to continue the editing cycle. These results confirmed that LL-DA-3 acted catalytically at the protein level, demonstrating superior performance compared to amino acid and small peptide systems. The enhanced editing efficiency highlighted the contribution of stronger protein-compound binding affinity (Supplementary Figs. S9 and S10).

Subsequently, we evaluated LL-DA-3 in a live-cell system. We expressed Flag-CDK2 in HEK-293T cells. After 2 hours (h) of light exposure that was preceded by LL-DA-3 incubation, cells were lysed and CDK2 was immunoprecipitated. LC-MS/MS analysis clearly detected the D145A-edited peptide with 10.07% efficiency (Fig. 1g), while the treatment induced detectable cellular stress (Supplementary Fig. S11), these results provide direct evidence that LL-DA-3 enables selective, site-specific protein editing within the intracellular environment and, importantly, that precise modification of a single carbon-carbon bond can be achieved even in a complex biological system.

To understand the structural basis for this efficiency and specificity, we solved the co-crystal structures of CDK2 bound to LL-DA-3 or LL-DA-4 (Fig. 1h; Supplementary Figs. S12, S13 and Table S6). Analysis of both structures reveals that LL-DA-3 and LL-DA-4 adopt highly similar bonding modes. LL-DA-3 occupies the ATP-binding pocket, where its 2-aminopyrimidine core forms hydrogen bonds with E83 in the hinge region. The guanidinium group, positively charged at physiological pH, forms electrostatic and hydrogen-bonding interactions with I10, Q131, and K89. A detailed analysis of the crystal structure of CDK2 in complex with LL-DA-3 reveals that the hydrogen bonding network involving conserved water molecules may play a crucial role (Supplementary Fig. S12c).

To probe the hydrodecarboxylation reaction within the CDK2 active site, we carried out quantum chemical calculations (Fig. 1i; Supplementary Fig. S14). These computations outline a photoreaction pathway initiated by photo-induced

electron transfer facilitated by hydrogen-bond rearrangement, particularly the movement of Wat172. The rearrangement promotes electron abstraction and decarboxylation. The reaction proceeds via intermediate M1 to a second transition state (TS2), involving a hydrogen atom transfer from K33 with a barrier of 10.19 kcal/mol, yielding intermediate M2. The final product state (P) is reached as the system relaxes to the ground state, with an overall Gibbs free energy change of +7.13 kcal/mol relative to the initial state (S), suggesting a thermodynamically favorable overall transformation.

In summary, we established LIDAPE, a modular platform that couples a light-induced 2-oxo-3-cyano photocatalytic warhead with a target-specific binder to enable site-selective D-to-A protein editing in complex biological settings, which theoretically allows for the selection of optimal warhead-binder combinations (Fig. 1j). The efficient conversion demonstrated on protein kinases with a well-defined ATP-binding pocket, such as CDK2, validates the feasibility of this platform and provides a preliminary proof of concept. Future studies may explore specific aspartate sites whose modification leads to significant physiological or pathological effects, with the potential to guide impactful biomedical engineering efforts, including vaccine design and immunotherapy. Moreover, prolonged exposure to short-wavelength light may induce protein oxidation and cellular damage, highlighting the demand for faster-editing, red-shifted LIDAPEs capable of dissecting signaling pathways, mimicking pathological mutations and engineering protein functions.

#### DATA AVAILABILITY

Coordinate files of presented models and crystal structures have been deposited in the wwPDB with accession numbers (9UAA and 9UAW).

#### ACKNOWLEDGMENTS

We thank the staffs from BL19U1 beamlines of National Facility for Protein Science in Shanghai (NFPS) at Shanghai Synchrotron Radiation Facility, for assistance during data collection. This work was partially supported by the National Key Research and Development Program of China (2022YF C3400500 to C.L.; 2025YFA1309400 and 2022YFA1302902 to H.Z.); Prevention and Control of Emerging and Major Infectious Diseases-National Science and Technology Major Project (2025ZD01903600; 2025ZD01903604 to H.L.); the National Natural Science Foundation of China (92253303 and U23A 20108 to C.L.; 22425703 to H.Z.; 22377013 to H.L.); the Science and Technology Commission of Shanghai Municipality (YDZX20233100004032 to C.L.), Major Program of Guangzhou National Laboratory (GZNL2023A02012 to C.L.), Shanghai Leading Talent Program of Eastern Talent Plan (LJ2023123 to H.Z.), the Strategic Priority Research Program

of the Chinese Academy of Sciences (XDB0830301 to C.L.; XDB0830000 to H.Z.); the Natural Science Foundation of Fujian Province (2023J01310 to J.L.); the Joint Funds for the Innovation of Science and Technology of Fujian Province (2023Y9017 to J.L.); Guizhou Province ([2024]015, SKLDFC-202504 and GMUSKL-202504 to C.L.).

#### AUTHOR CONTRIBUTIONS

H.L. and C.L. designed the study. J.Y., Y.B. and H.L. conducted compound synthesis. J.L. screened catalysts. Y.H. and F.Y. performed quantum chemistry calculations. Z.W., Z.L. and J.Q. performed protein purification. G.S. designed the biological experiments. S.F. obtained the co-crystal structure of the compound-CDK2. Z.Y., Y.M. and H.Z. analyzed the mass spectrometry data. G.S., J.L., Z.Y., F.Y., H.L. and C.L. wrote the manuscript.

#### COMPETING INTERESTS

The authors declare no competing interests.

#### REFERENCES

- Cong, L. et al. *Science* **339**, 819–823 (2013).
- Mali, P. et al. *Science* **339**, 823–826 (2013).
- Doudna, J.A. *Nature* **578**, 229–236 (2020).
- Beyer, J.N. et al. *Science* **388**, eadr5499 (2025).
- Hua, Y. et al. *Science* **388**, 68–74 (2025).
- Josephson, B. et al. *Nature* **585**, 530–537 (2020).
- Ting, C.P. et al. *Science* **365**, 280–284 (2019).
- Cohen, P., Cross, D. & Jänne, P.A. *Nat. Rev. Drug. Discov.* **20**, 551–569 (2021).
- Attwood, M.M., Fabbro, D., Sokolov, A.V., Knapp, S. & Schiöth, H.B. *Nat. Rev. Drug. Discov.* **20**, 839–861 (2021).
- Adams, J.A. *Chem. Rev.* **101**, 2271–2290 (2001).
- Bloom, S. et al. *Nat. Chem.* **10**, 205–211 (2018).
- Sorigué, D. et al. *Science* **372**, eabd5687 (2021).
- Shinkawa, Y. et al. *J. Org. Chem.* **87**, 11816–11825 (2022).
- Sun, G. et al. *Angew. Chem. Int. Ed.* **64**, e202513542 (2025).
- Zhang, Z.M. et al. *Nat. Commun.* **15**, 6477 (2024).

#### ADDITIONAL INFORMATION

**Supplementary information** The online version contains supplementary material available at <https://doi.org/10.15302/vita.2026.03.0020>.

**Correspondence** and requests for materials should be addressed to Hu Zhou, Hua Lin or Cheng Luo.

**Reprints and permission information** is available at <https://www.vita-journal.com/>.

© The Author(s) 2026. Published by Higher Education Press. This is an Open Access article distributed under the terms of the CC BY license (<https://creativecommons.org/licenses/by/4.0/>).